THE USE OF HAMILTONIAN DYNAMICS IN THE GLOBAL ANALYSIS OF SYSTEMS LIABLE TO UNSTABLE POST-BUCKLING BEHAVIOR

Orlando, Diego
Gonçalves, Paulo Batista
Department of Civil Engineering, Catholic University, PUC-Rio, 22451-900, Rio de Janeiro, RJ, Brazil.
dorlando@aluno.puc-rio.br
paulo@puc-rio.br

Rega, Giuseppe
Dipartimento di Ingegneria Strutturale e Geotecnica, Sapienza Università di Roma, 00197, Roma, Italy.
giuseppe.rega@uniroma1.it

Lenci, Stefano
Dipartimento di Architettura, Costruzioni e Strutture, Università Politecnica delle Marche, 60131, Ancona, Italy.
lenci@univpm.it

Abstract. *The prevention of buckling is a major concern in engineering design. This is particularly important in the analysis of systems liable to unstable post-buckling behavior. In these systems, for applied loads lower than the theoretical buckling load the system is supposedly in a safe position. However this is not completely true. The system may buckle at load levels much lower than the critical value due to the simultaneous effects of imperfections and dynamic disturbances. The imperfections decrease the theoretical buckling load and at the same time change the topology of the potential energy of the system, changing consequently its global dynamic behavior and stability. For systems liable to unstable post-buckling behavior, the safe pre-buckling well is delimited by the saddles associated with the unstable post-buckling path. The heteroclinic or homoclinic orbits emerging from these saddles define the safe region. In the present paper, methods of Hamiltonian dynamical systems theory are applied to some simple well-known mechanical models that exhibit unstable post-buckling behavior. Particular attention is given to the analysis of Augusti's model where mode interaction leads to high imperfection sensitivity and a complex dynamics. The aim of this paper is to show that the tools of Hamiltonian dynamics, applied in the manner described, leads to a useful description of the imperfection sensitivity and integrity of the structure. A qualitative geometric picture of the underlying dynamics emerges which itself proves to be suitable for the extraction of possibly quantitative information, without recourse to lengthy algebraic manipulations or computer-intensive numerical simulations.*

Keywords*: buckling, unstable-post-buckling, Hamiltonian dynamics, escape, global stability*

1. INTRODUCTION

The seminal work on the modern post-buckling analysis of structures is due to Koiter (1967) who first studied through a perturbation approach the initial post-buckling behavior of structural systems and the effect of geometric imperfections on their nonlinear structural response and load-carrying capacity. Koiter's initial post-buckling theory was further developed by, among others, Chilver (1972), Croll and Walker (1972) and Thompson and Hunt (1973) in England and by Budiansky (1974) and Hutchinson (1974) in USA. These works set the basis of the modern theory of structural stability (El Naschie, 1990; Bazant and Cedolin, 1991). The main merit of this theory is to explain how the post-buckling analysis can help in the explanation of the complex non-linear response of real structures. This is particularly important in the analysis of systems liable to unstable buckling. In such cases, the load-carrying capacity of the structure in governed by the unstable branches of the post-buckling response. Also, in these structures the imperfections may substantially decrease the load capacity of the structure and the choice of a safe load level for design becomes usually a complex and difficult task for the engineer. The nonlinear analysis of the imperfect structure may help the engineer in the design process. However, most of the studies in this area relies on the local stability analysis of an equilibrium configuration and no additional information is given on the safety of a given equilibrium state. The aim of the present work is to show that a global stability analysis using the mathematical methods of classical mechanics, in particular Lagrangian or Hamiltonian mechanics can help the engineer in the understanding of this problem.

The fundamentals of Lagrangian and Hamiltonian mechanics and their application to the analysis of discrete mechanical systems can be found in, for example, the works of Arnold (1989), Greenwood (2003) and Meirovitch (2003). Using these tools one can analyze the dynamic behavior of the undamped or lightly damped structural system and obtain, using relatively simple mathematical tools, a picture of the global dynamics and how the unstable post-buckling solutions limit the range of possible disturbances. This link between nonlinear dynamics and structural stability is illustrated in Figure 1, where the three possible post-buckling responses of a perfect conservative sdof structural system are shown schematically together with the evolution of the global phase space as a function of the static applied load (El Naschie, 1990; Thompson and Hunt, 1984). From the structural engineering point of view, the

three distinct local bifurcations associated with three distinct branching points are the stable symmetric, the unstable symmetric and the asymmetric. There is also the limit point instability. For the stable case, one can see that mathematically any disturbance, independent of its magnitude, will lead to an orbit around the stable equilibrium point (a center). This remains unchanged up to the critical load, where the fundamental solution becomes unstable giving rise to two centers corresponding to the two stable symmetric post-buckling configurations and a saddle, corresponding to the trivial solution. For the unstable symmetric case, there are for load levels lower than the critical load two saddles associated with the unstable post-buckling configurations and a center corresponding to the stable pre-buckling state. In this case the maximum magnitude of the disturbances that lead to bounded solutions around the stable point is limited by the two heteroclinic orbits that connect the two saddles. This region decreases as the load increases and vanishes at the critical point. A similar behavior is observed in the asymmetric case (and also in the limit point case). But here there are for load levels lower that the critical load one center and one saddle and the stable region is limited by the homoclinic orbit of the saddle. Introducing some small damping to the essentially Hamiltonian, conservative systems, the three centers become attractors (focuses or nodes, depending on the damping coefficient and load level, (Thompson and Stewart, 1987)). If in the two latter cases the disturbances are higher than those limited by the heteroclinic or homoclinic orbits the responses diverge to infinity. This is termed escape from the pre-buckling potential well.

The understanding of the global behavior of structures subjected to unstable post-buckling behavior is particularly important in structural systems where modal interaction of different buckling modes with equal or nearly equal buckling loads may lead to new unstable and sometimes unexpected equilibrium paths. This has been observed in several structural systems such as bars, plates and shells (Tvergaard, 1973; Kiymaz, 2005; Teng *et al.,* 2006, Quin *et al.*, 2007; Kolakowski, 2007; Dinis et al, 2007). An archetypal model of such systems is the well known two dof Augusti's model (Bazant and Cedolin, 1991; Del Prado, 1999; Raftoyiannis and Kounadis, 2000). Other simplified models displaying the same behavior are found in literature (Thompson and Gaspar, 1977; Jansen, 1977; Hunt *et al.*, 1979; Thompson and Hunt, 1984; El Naschie, 1990; Sophianopoulos, 2007).

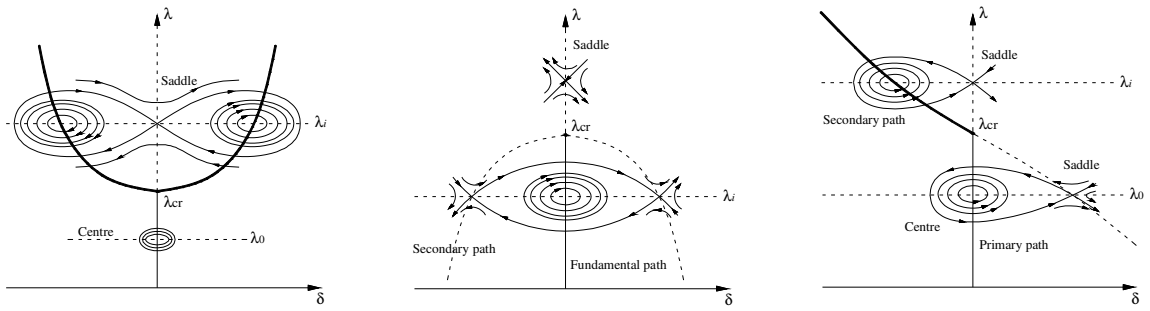

(a) Symmetric stable (b) Symmetric unstable (c) Asymmetric

Figure 1. The three points of bifurcation. Phase space transformation along the fundamental and secondary paths of sdof structural systems (El Naschie, 1990)

2. FORMULATION OF THE PROBLEM

Figure 2 illustrates the Augusti's model. It is an inverted spatial pendulum composed of a slender, rigid (but massless) bar of length l, with a tip-mass m, pinned at the base, where two rotational springs with constant stiffness k_1 and k_2 initially act in perpendicular planes and rotate with the bar. The angles θ_1 and θ_2 are chosen as the two degrees of freedom.

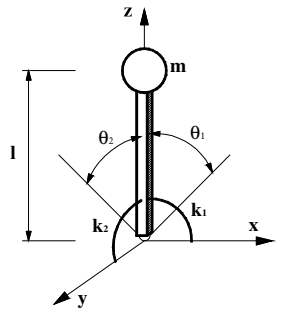

Figure 2. Augusti´s two-degree-of-freedom model.

The total potential energy of the system is given by

$$\overline{V} = \frac{V}{ml^2} = \frac{1}{2}\frac{\omega_p^{\,2}}{\lambda}\theta_1^{\,2} + \frac{1}{2}\frac{\omega_p^{\,2}}{\lambda}\theta_2^{\,2} - \omega_p^{\,2}(1 - \sqrt{1 - \sin^2\theta_1 - \sin^2\theta_2}) \tag{1}$$

where $P = mg$, while the kinetic energy is written as

$$\overline{T} = \frac{T}{ml^2} = \frac{1}{2}\left(\dot{\theta}_1^{\,2}\cos^2\theta_1 + \dot{\theta}_2^{\,2}\cos^2\theta_2 + \frac{\left(\dot{\theta}_1\cos\theta_1\sin\theta_1 + \dot{\theta}_2\cos\theta_2\sin\theta_2\right)^2}{\cos^2\theta_1 + \cos^2\theta_2 - 1}\right) \tag{2}$$

Lagrangian mechanics describes the motion of a mechanical system by means of its configuration space. In mechanics, the function

$$L(\theta_i, \dot{\theta}_i) = \overline{T} - \overline{V} = \frac{1}{2}\left(\dot{\theta}_1^{\,2}\cos^2\theta_1 + \dot{\theta}_2^{\,2}\cos^2\theta_2 + \frac{\left(\dot{\theta}_1\cos\theta_1\sin\theta_1 + \dot{\theta}_2\cos\theta_2\sin\theta_2\right)^2}{\cos^2\theta_1 + \cos^2\theta_2 - 1}\right) - \frac{1}{2}\frac{\omega_p^{\,2}}{\lambda}\theta_1^{\,2} - \frac{1}{2}\frac{\omega_p^{\,2}}{\lambda}\theta_2^{\,2} + \omega_p^{\,2}(1 - \sqrt{1 - \sin^2\theta_1 - \sin^2\theta_2}) \tag{3}$$

is known as Lagrange function or Lagrangian. Here θ_i are the generalized coordinates, $\dot{\theta}_i$, the generalized velocities, $\partial L / \partial \dot{\theta}_i = p_i$, the generalized momenta and $\partial L / \partial \theta_i = \dot{p}_i$, the generalized forces, $\lambda = P/Pcr$, $\omega_p^2 = g/l$, $k/ml^2 = \omega_p^2/\lambda$, $k_1 = k_2 = k$ and $Pcr_1 = Pcr_2 = Pcr = k/l$.

The equations of motion of the system are obtained, using Hamilton´s principle of least action, as the extremals of the functional $\Phi = \int_{t_1}^{t_2} L dt$, known as the action. Then the evolution of θ_i with time is subjected to the Euler-Lagrange equations of motion:

$$\frac{d}{dt}\frac{\partial(\overline{T})}{\partial\dot{\theta}_i} - \frac{\partial(\overline{T})}{\partial\theta_i} + \frac{\partial(\overline{V})}{\partial\theta_i} = 0 \tag{4}$$

So, for Augusti´s model the following equations of motion in terms of the generalized coordinates θ_1 and θ_2, are given explicitly by

$$\begin{aligned} & ml^2\left(\ddot{\theta}_1(-\cos^2\theta_1\cos^2\theta_2 + \cos^4\theta_1\cos^2\theta_2 + \cos^2\theta_1\cos^4\theta_2) + \ddot{\theta}_2(-\cos\theta_1\sin\theta_1\cos\theta_2\sin\theta_2 + \right. \\ & \cos^3\theta_1\sin\theta_1\cos\theta_2\sin\theta_2 + \cos\theta_1\sin\theta_1\cos^3\theta_2\sin\theta_2) + \dot{\theta}_1^{\,2}(-\cos\theta_1\sin\theta_1\cos^4\theta_2 + \cos\theta_1\sin\theta_1\cos^2\theta_2) + \\ & \dot{\theta}_2^{\,2}(\cos\theta_1\sin\theta_1 - 2\cos\theta_1\sin\theta_1\cos^2\theta_2 - \cos^3\theta_1\sin\theta_1 + 2\cos^3\theta_1\cos^2\theta_2\sin\theta_1 + \cos\theta_1\cos^4\theta_2\sin\theta_1) + \\ & \left.\dot{\theta}_1\dot{\theta}_2(2\cos^2\theta_1\cos\theta_2\sin\theta_2 - 2\cos^4\theta_1\cos\theta_2\sin\theta_2)\right) + \left(\frac{\omega_p^{\,2}}{\lambda}\theta_1 - \omega_p^{\,2}\frac{\cos\theta_1\sin\theta_1}{\sqrt{1 - \sin^2\theta_1 - \sin^2\theta_2}}\right)(1 - 2\cos^2\theta_1 - \\ & 2\cos^2\theta_2 + \cos^4\theta_1 + \cos^4\theta_2 + 2\cos^2\theta_1\cos^2\theta_2) = 0 \end{aligned} \tag{5}$$

$$ml^2\Big(\ddot{\theta}_2(-\cos^2\theta_1\cos^2\theta_2+\cos^4\theta_1\cos^2\theta_2+\cos^2\theta_1\cos^4\theta_2)+\ddot{\theta}_1(-\cos\theta_1\sin\theta_1\cos\theta_2\sin\theta_2+$$
$$\cos^3\theta_1\sin\theta_1\cos\theta_2\sin\theta_2+\cos\theta_1\sin\theta_1\cos^3\theta_2\sin\theta_2)+\dot{\theta}_2^{\,2}(-\cos^4\theta_1\cos\theta_2\sin\theta_2+\cos^2\theta_1\cos\theta_2\sin\theta_2)+$$
$$\dot{\theta}_1^{\,2}(\cos\theta_2\sin\theta_2-2\cos^2\theta_1\cos\theta_2\sin\theta_2-\cos^3\theta_2\sin\theta_2+2\cos^2\theta_1\cos^3\theta_2\sin\theta_2+\cos^4\theta_1\cos\theta_2\sin\theta_2)+ \quad (6)$$
$$\dot{\theta}_1\dot{\theta}_2(2\cos\theta_1\sin\theta_1\cos^2\theta_2-2\cos\theta_1\sin\theta_1\cos^4\theta_2)\Big)+\left(\frac{\omega_p^{\,2}}{\lambda}\theta_2-\omega_p^{\,2}\frac{\cos\theta_2\sin\theta_2}{\sqrt{1-\sin^2\theta_1-\sin^2\theta_2}}\right)(1-2\cos^2\theta_1-$$
$$2\cos^2\theta_2+\cos^4\theta_1+\cos^4\theta_2+2\cos^2\theta_1\cos^2\theta_2)=0$$

The system of Lagrange's equations is equivalent to the system of *2n* first-order equations, known as Hamilton's equations

$$\dot{p}_i=-\frac{\partial H}{\partial\theta_i},\qquad \dot{\theta}_i=\frac{\partial H}{\partial p_i},\qquad i=1,2 \quad (7)$$

where *H* is the Hamiltonian function, which, based on Legendre dual transform, can be written as

$$H=p_1\dot{\theta}_1+p_2\dot{\theta}_2-L \quad (8)$$

For Augusti's model one obtains

$$H=p_1\left(p_2-p_1\frac{\sin\theta_1\sin\theta_2}{\cos\theta_1\cos\theta_2}\right)+p_2\left(p_1-p_2\frac{\sin\theta_1\sin\theta_2}{\cos\theta_1\cos\theta_2}\right)-\frac{1}{2}\left(\left(p_2-p_1\frac{\sin\theta_1\sin\theta_2}{\cos\theta_1\cos\theta_2}\right)^2\cos^2\theta_1+\right.$$
$$\left.\left(p_1-p_2\frac{\sin\theta_1\sin\theta_2}{\cos\theta_1\cos\theta_2}\right)^2\cos^2\theta_2+\frac{\left(\left(p_2-p_1\frac{\sin\theta_1\sin\theta_2}{\cos\theta_1\cos\theta_2}\right)\cos\theta_1\sin\theta_1+\left(p_1-p_2\frac{\sin\theta_1\sin\theta_2}{\cos\theta_1\cos\theta_2}\right)\cos\theta_2\sin\theta_2\right)^2}{\cos^2\theta_1+\cos^2\theta_2-1}\right)+$$
$$\frac{1}{2}\frac{\omega_p^{\,2}}{\lambda}\theta_1^{\,2}+\frac{1}{2}\frac{\omega_p^{\,2}}{\lambda}\theta_2^{\,2}-\omega_p^{\,2}\left(1-\sqrt{1-\sin^2\theta_1-\sin^2\theta_2}\right) \quad (9)$$

This shows the equivalence of Lagrange's and Hamilton's equations (Arnold, 1989). For a mechanical system where the Lagrangian is given by Eq. 3, and *T* is a quadratic function of the generalized velocities, the Hamiltonian *H* is the total energy of the system, that is, $H=2T-(T-V)=T+V$.

The Lagrange equations of motion constitute a set of *n* second-order differential equations with *2n* constants of integration. If the problem can be solved completely in terms of known elementary functions or indefinite integrals, it is called a problem soluble by quadratures. This is the case when the system admits the first integrals of motion. These integrals are written in terms of the generalized coordinates and velocities or, alternatively, in terms of the generalized coordinates and associated momenta. These integrals enable one to derive a large number of information about the behavior of the system without actually obtaining a complete solution of the equations of motion.

If the mechanical system is a conservative system, that is, if all generalized forces are obtained by deriving a potential function that is a function of the generalized coordinates only and not an explicit function of time, then the total energy of the system is constant. This constitutes in this case the first integral of motion.

3. Behavior of Augusti's Model

In the following the static and dynamic behavior of the conservative 2 dof model is discussed.

3.1. Stability Analysis and Safe Pre-Buckling Region

Considering $k_1=k_2=k$, Augusti´s model displays two coincident buckling loads, $Pcr_1=Pcr_2=Pcr=k/l$, and orthogonal buckling modes $\theta_1\{1,0\}$ and $\theta_2\{0,1\}$. The non-linear post-buckling behavior in this case can be described by the following set of two coupled non-linear equations

$$\theta_1 - \lambda \frac{\cos\theta_1 \sin\theta_1}{\sqrt{1-\sin^2\theta_1 - \sin^2\theta_2}} = 0 \tag{10}$$

$$\theta_2 - \lambda \frac{\cos\theta_2 \sin\theta_2}{\sqrt{1-\sin^2\theta_1 - \sin^2\theta_2}} = 0 \tag{11}$$

Figure 3 shows the fundamental path ($\theta_1 = \theta_2 = 0$), which is stable up to the static critical load ($\lambda = 1$) and the four possible post-buckling paths: the two ascending unstable paths, which correspond to the two uncoupled solutions (either θ_1 or θ_2 is zero) and the two descending unstable orthogonal paths at 45°, which are the solutions of the coupled system (10-11). The interaction of the buckling modes leads to increased imperfection sensitivity. If, for example, k_1 is much less than k_2, only one stable post-buckling ascending path emerges at $Pcr_1 = k_1 / l$, and the problem is imperfection insensitive. The important fact to note is that interaction of the buckling modes θ_1 and θ_2 conspires to produce the descending unstable paths and imperfection sensitivity, although each mode taking place alone exhibits no imperfection sensitivity (Bazant and Cedolin, 1991; Van der Heijden, 2008).

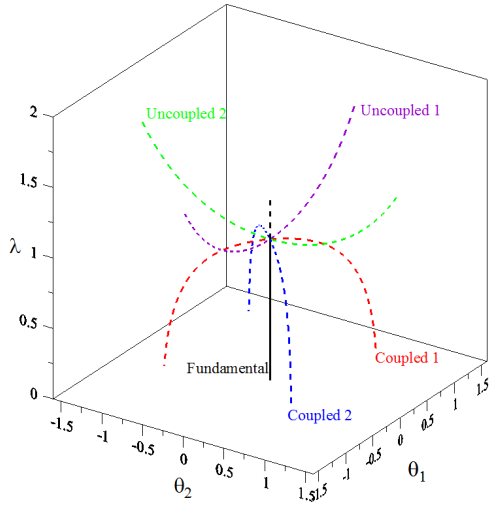

Figure 3. Equilibrium paths of the system.

Figure 4, where the potential energy surface, expression (1), and its projection onto the θ_1 vs. θ_2 plane is shown for $\lambda = 0.3$, $\lambda = 0.9$ and $\lambda = 1.25$, illustrates the variation of the potential energy with the static load levels. Figures 4(a) and 4(b) show that, for values of λ between zero and the critical load, there is one local minimum, corresponding to the stable pre-buckling solution, surrounded by four saddles at the same energy level. The four saddles are associated with the unstable equilibrium paths corresponding to the coupled solutions. So, due to the modal coupling, for static load levels lower than the critical load the system may loose stability by escaping from the pre-buckling well if any external perturbation exceeds the safe region delimited by the four saddles. This safe region decreases as the static load increases and becomes zero at the critical load. Figure 4(c) shows the potential energy for $\lambda = 1.25$, a value higher than the critical load ($\lambda_{cr} = 1.00$). In this case, after the critical load, both eigenvalues change sign simultaneously and the local minimum associated with the trivial solution is transformed into a local maximum. Four saddles associated with the uncoupled post-buckling solutions are also observed in Figure 4(c). The potential energy landscape gives the engineer a global picture of the problem and shows how the unstable solutions influence the safety of the system. As the load increases and the stable region decreases the range of allowable disturbances decreases accordingly. So, near a bifurcation point even very small perturbation may lead to escape from the pre-buckling well. Since all structures work in a dynamical environment a safety factor must be used in design. Since structural systems are usually lightly damped, the response of the real structure will only depart lightly from the conservative case.

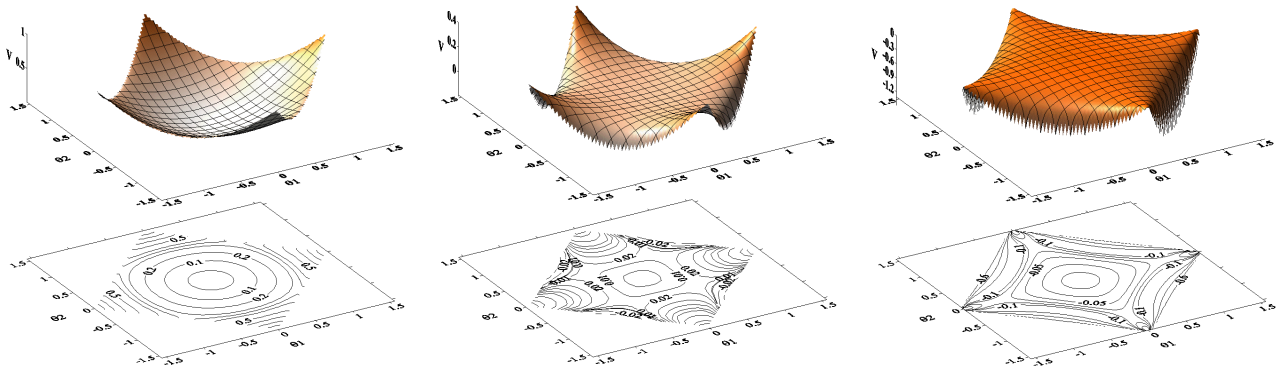

(a) $\lambda = 0.3$ (b) $\lambda = 0.9$ (c) $\lambda = 1.25$

Figure 4. Curves of equal potential energy.

If Augusti's model had been modeled as a sdof model moving in one of the uncoupled planes, it would exhibit a solution similar to that shown in Figure 1(a) and no escape would occur for load levels lower than the critical load. This is a serious point that should be considered in the mathematical modeling of certain structural problems. If all possible modal couplings are not taken into account, the designer may obtain a completely wrong description of the problem leading to a faulty and potentially unsafe design.

Much of the global behavior and dynamics of a structural system can be understood from the topologic structure of its potential and total energy functions. However, in a high-dimensional conservative dynamical system, it is difficult to make direct analysis of the geometrical structure of the phase space and the high-dimensional basin boundary. Safe basins are objects of the same dimension of the phase space, four-dimensional in our case. Therefore they cannot be fully visualized here. Useful insight can however be derived from observation of two- and three-dimensional cross-sections and from the geometry of the stable and unstable manifolds emerging from the saddles. The four heteroclinic orbits that connect the four symmetric saddles shown in Figure 5, for $\lambda = 0.9$, separate the initial conditions that lead to bounded solutions surrounding the pre-buckling configuration from the unbounded escape solutions. The knowledge of these frontiers helps the designer to separate the phase space into safe and unsafe domains.

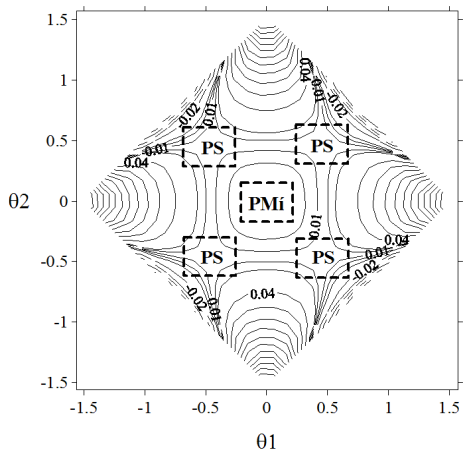

Figure 5. Curves of equal potential energy for $\lambda = 0.9$. PS: Saddles. PMi: Stable position corresponding to a local minimun.

So, the four heteroclinic orbits lie on a hypersurface that bounds the initial conditions leading to bounded solutions around the trivial pre-buckling solution, that is, the interior of this region is filled with a continuous family of stable trajectories. The equation of this surface can be obtained by the conservation of the total energy principle, equating the sum of expressions (1) and (2) to the value of the total energy at one of the saddles, that is

$$T(\theta_i, \dot{\theta}_i) + V(\theta_i) = C_{saddle} \tag{12}$$

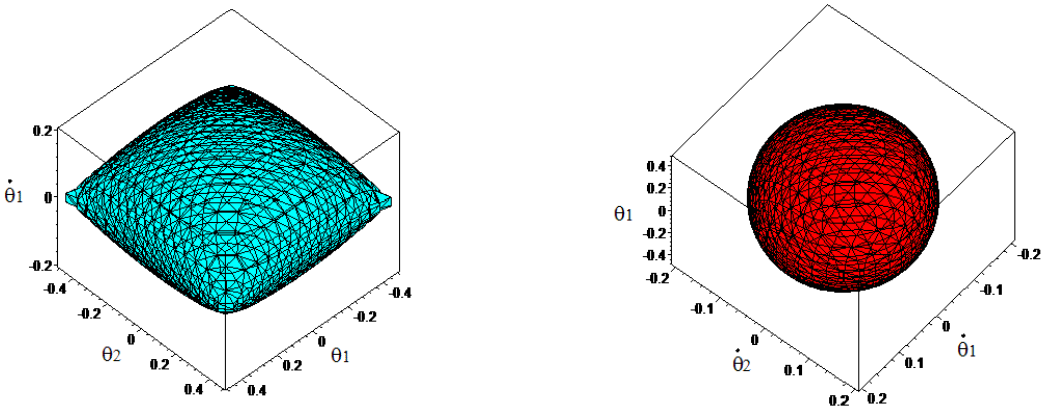

(a) Plane $\theta_1\theta_2 d\theta_1/dt$ (b) Plane $d\theta_1/dtd\theta_2/dt\theta_1$

Figure 6. Two three-dimensional sections of safe pre-buckling region. $\lambda = 0.9$ and $\omega_p = 1$.

Two three-dimensional and four two-dimensional sections of this four-dimensional region are shown in Figure 6 and Figure 7, respectively, for a given value of the pendulum natural frequency ω_p. Four projections of the stable and unstable manifolds of the four saddles that lie on the hyper-surface defined by Eq. (12) and defines the safe region are shown in Figure 8. As one can observe, the safe region is bounded by four heteroclinic orbits. This 4D region is defined as the conservative safe basin of the pre-buckling configuration. This safe hyper-volume decreases swiftly in all planes as the static load increases and vanishes at the critical point. An analysis of this region gives information on the maximum allowed displacements and velocities. They also can help in vibration control by giving the upper bound of allowable disturbances.

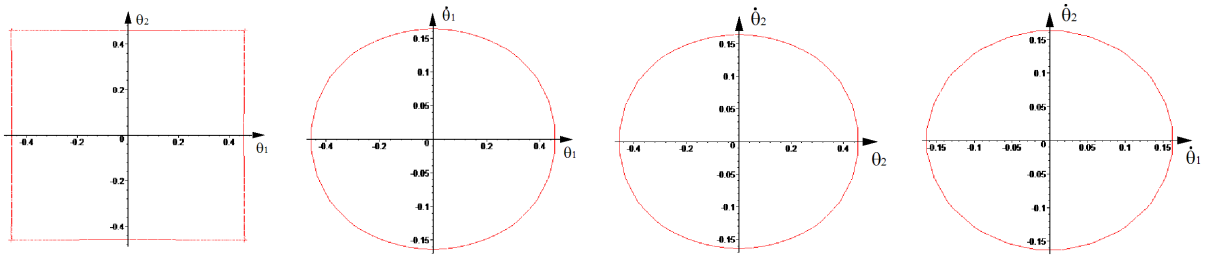

(a) Plane $\theta_1\theta_2$ (b) Plane $\theta_1 d\theta_1/dt$ (c) Plane $\theta_2 d\theta_2/dt$ (d) Plane $d\theta_1/dtd\theta_2/dt$

Figure 7. Four two-dimensional sections of safe pre-buckling region. $\lambda = 0.9$ and $\omega_p = 1$.

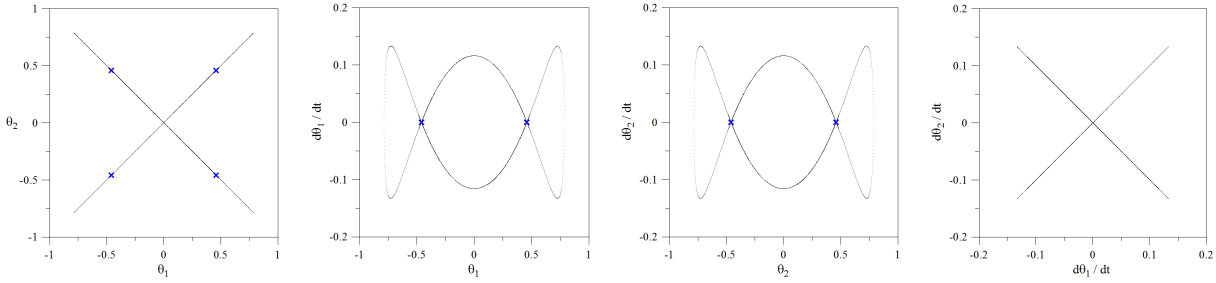

(a) $\theta_1\theta_2$ (b) $\theta_1 d\theta_1/dt$ (c) $\theta_2 d\theta_2/dt$ (d) $d\theta_1/dtd\theta_2/dt$

Figure 8. Four two-dimensional projections of the stable and unstable manifold of the four saddles. $\lambda = 0.9$ and $\omega_p = 1$.

3.2. Free Vibration Analysis

Considering $k_1 = k_2 = k$, Augusti´s model also displays two coincident free vibration frequencies, $\omega_1 = \omega_2 = \omega_p \sqrt{[(1/\lambda) - 1]}$, and orthogonal, uncoupled, linear vibration modes .

The dynamic behavior of the conservative perturbed system is also an important tool in the analysis of systems liable to unstable post-buckling behavior. The results in the previous sections show that the potential energy is highly distorted, departing from that of the linearized system. Thus the energy level, associated with a given set of initial conditions has a remarkable influence on the vibrations of the perturbed system. From Eq. 9, one can observe that at the stable equilibrium point the total energy is zero. As the energy level increases and approaches that related to the saddles, the complexity of the free vibrations of the system increases. This can be studied by Poincaré maps of the four-dimensional flow. By fixing the total energy of the system to a constant level, one restricts the flow of the dynamical system to an isoenergetic 3-dimensional manifold. This is achieved by setting $H=h$, where h is a constant energy level. If the 3-dimensional isoenergetic manifold, is cut by a 2-dimensional plane and if the intersection of the two manifolds is transverse (Guckenheimer and Holmes, 1984; Vakakis, 1991), the resulting cross section $\sum$ is 2-dimensional, and the flow of the dynamical system intersecting the cut-plane defines a Poincaré map. Here the cut-plane is chosen as $\Pi = \{\theta_2 = 0\}$ and the Poincaré section $\sum$ is defined by:

$$\sum = \{\theta_2 = 0, \dot{\theta}_2 > 0\} \cap \{H = h\} \tag{13}$$

The restriction on the velocity is because the Poincaré map must be orientation preserving (Guckenheimer and Holmes, 1984; Vakakis, 1991).

Using Eqs. (1) and (2) to evaluate $H=h$, the initial condition $\dot{\theta}_2$ corresponding to a given initial pair $(\theta_1, \dot{\theta}_1)$ is obtained as:

$$\dot{\theta}_2 = \pm\sqrt{-\dot{\theta}_1^2 - \frac{\omega_p^2}{\lambda}\theta_1^2 + 2\omega_p^2(1-\cos\theta_1) + 2h} \tag{14}$$

where the sole positive value holds. The interior region filled by the points $(\theta_1, \dot{\theta}_1)$ is defined by positive values of the radicand in Eq. (14), so that the boundary of this region is defined by the condition that the radicand vanishes, which yields:

$$h = \frac{1}{2}\dot{\theta}_1^2 + \frac{1}{2}\frac{\omega_p^2}{\lambda}\theta_1^2 - \omega_p^2(1-\cos\theta_1) \tag{15}$$

The dynamics inside this region is obtained by integrating Eqs. (5) and (6) for various initial conditions of $(\theta_1, \dot{\theta}_1)$, based on the above restrictions on θ_2 and $\dot{\theta}_2$.

Figure 9 shows three Poincaré maps of the system for h=0.00001345, 0.005, 0.0134556, corresponding to low, medium and high energy levels. For zero energy level the cross-section reduces to a point that corresponds to the uncoupled vibration mode in the $(\theta_2, \dot{\theta}_2)$ plane. However for even a small energy level (see Figure 9(a) for $h = 0.00001345$ and the inset zoomed region of the central phase-space), although the origin continues to be stable, one can observe clearly the appearance of two saddles and two centers, which correspond to four new free vibration modes, two stable and two unstable. The two stable modes correspond to similar nonlinear modes due to the modal coupling with the system vibrating with θ_1 and θ_2 in phase and with θ_1 and θ_2 out-of-phase. The same can be observed in Figure 9(b) for $h = 0.005$. The heteroclinic orbits of the two saddles divide the region defined by Eq. (15) into four sub-regions. Depending on the initial conditions, there are quasiperiodic motions about the origin ($\theta_1 = \dot{\theta}_1 = 0$), which corresponds to the uncoupled vibration mode in the $(\theta_2, \dot{\theta}_2)$ plane, quasiperiodic motions around the two eminently nonlinear vibration modes and large amplitude quasiperiodic vibrations around the three centers. The third energy level, $h = 0.0134556$, corresponds to the energy level of the four saddles in Figure 5, which is the highest energy level meaningful for the present stability analysis. In Figure 9(c) a rather complex dynamics is observed within the interior region, with diffuse sets of points which indicate random-like chaotic dynamics. It is worth noting how the region wherein the dynamics is confined coincides just with the two-dimensional section of the four-dimensional safe pre-buckling region shown in Fig. 7(b). For higher values of h, the response associated to any nontrivial set of initial conditions diverges to infinity. One must keep in mind that traditional perturbation techniques are not able to detect most of the phenomena observed numerically for medium and large energy levels. However, even at this energy level,

there exist regions where regular free oscillations occur. The meaning of low and high energy levels depends on the nonlinear dynamical system and the departure of the nonlinear potential energy from the quadratic potential (linearized system), as illustrated in Figure 10 for a cross section of the potential energy shown in Figure 4(b) along the diagonal $\theta_1 = \theta_2$. Due to the double symmetry of the structural system, Poincaré sections similar to those shown in Figure 9 are obtained in the in the (θ_2 , $\dot{\theta}_2$) plane, where the origin corresponds to the uncoupled vibration mode in the in the ($\theta_1, \dot{\theta}_1$) plane.

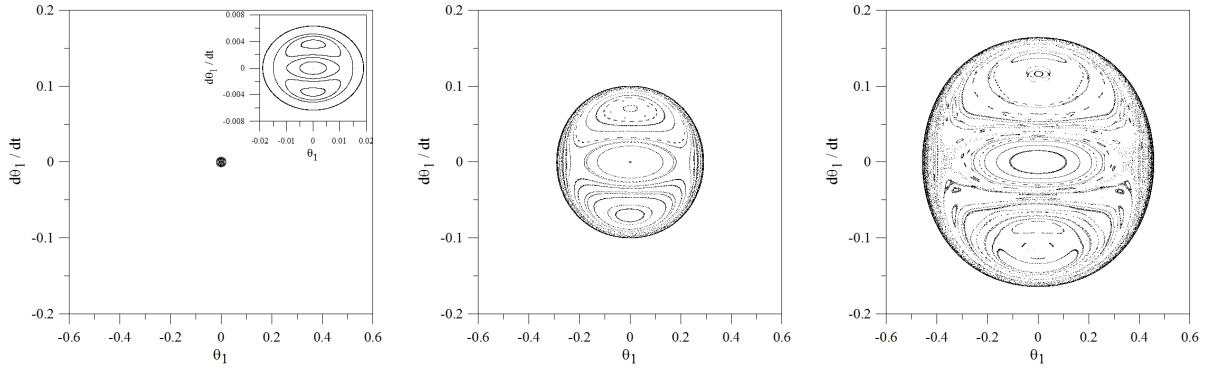

(a) h = 0.00001345 (b) h = 0.005 (c) h = 0.0134556

Figure 9. Poincaré maps of the system for low to high energy levels. $\lambda = 0.9$ and $\omega_p = 1$.

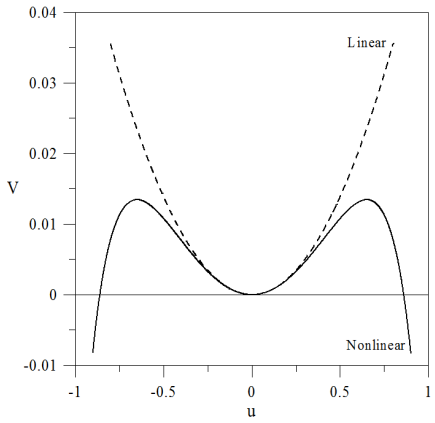

Figure 10. Comparison of the potential energy of the fully nonlinear problem with that of the linearized system (quadratic potential function). Cross section along the axis $\theta_1 = \theta_2$.

4. CONCLUSIONS

This paper analyses the global static and dynamic behavior of Augusti's model and shows how the tools of Hamiltonian dynamics can give the engineer a satisfactory understanding of the safety and integrity of the model. This analysis can be extended to any discrete system liable to unstable post-buckling behavior.

5. ACKNOWLEDGEMENTS

The authors acknowledge the financial support of the Brazilian research agencies CAPES, CNPq and FAPERJ.

6. REFERENCES

Arnold, V. I. 1989 Mathematical Methods of Classical Mechanics, 2nd Ed., Springer, New York, USA

Bazant, Z.P. and Cedolin, L., 1991, "Stability of Structures", Oxford Press, Oxford, UK.

Budianky, B. 1974 Theory of Buckling and Post-Buckling Behavior of Elastic Structures, Advances in Applied Mechanics, Vol. 14, Academic Press

Chilver, A. H. 1972 The Elastic Stability of Structures, In: Leipholz, H.H. Ed. Stability, Chapter 3, Solid Mechanics Division, University of Waterloo Press, Canadá.

Croll, J. G. and Walker, A. C. 1972 Elements of Structural Stability 1st Ed. Macmillan, London, UK

Del Prado, Z.J.G.N., 1999, "Vibrações Não Lineares e Instabilidade Dinâmica de Estruturas Sujeitas a Interação Modal", Proposta de Tese – PUC-Rio, Rio de Janeiro, Brasil.

Dinis, P.B., Camotim, D. and Silvestre, N., 2007, "FEM-Based Analysis of the Local-Plate/Distortional Mode Interaction in Cold-Formed Steel Lipped Channel Columns", *Computers & Structures*, Vol. **85** (19-20), pp. 1461-1474.

El Naschie, M.S., 1990, "Stress, Stability and Chaos in Structural Engineering: an Energy Approach", McGraw Hill, London, UK.

Greenwood, D. T. 2003 Advanced Dynamics, Cambridge University Press, Cambridge, UK

Guckenheimer, J. and Holmes, P. 1984 Nonlinear Oscillations, Dynamical Systems and Bifurcations of Vector Fields, Springer-Verlag, New-York, USA

Hunt, G.W., Reay, N.A. and Yoshimura, T., 1979, "Local Diffeomorphisms in the Bifurcational Manifestations of the Umbilic Catastrophes", Proc. R. Soc. Lond., A, Vol. 369, pp. 47-65.

Hutchinson, J. W., 1974, Plastic Buckling, Advances in Applied Mechanics, Vol. 14, Academic Press

Jansen, J.S., 1977, "Some Two-Mode Buckling Problems and Their Relation to Catastrophe Theory", AIAA Journal, Vol. 15 (11), pp. 1638.

Kiymaz, G., 2005, "FE Based Mode Interaction Analysis of Thin-Walled Steel Box Columns Under Axial Compression", *Thin-Walled Structures*, Vol. **43** (7), pp. 1051-1070.

Koiter, W. T. 1967 On the Stability of Elastic Equilibrium Nasa Report no TT-F-10833 (Translation of: Over Stabiliteit van het Elastiche Evenwitch, Ph. D. Thesis, Delft, ND, 1945)

Kolakowski, Z. 2007, "Some Aspects of Dynamic Interactive Buckling of Composite Columns", *Thin-Walled Structures*, In Press, Corrected Proof

Meirovitch, L., 2003, "Methods of Analytical Dynamics", Dover, New York, USA.

Quin, D.D., Wilber, J.P., Clemons, C.B., Young, G.W. and Buldum, A., 2007, "Buckling Instabilities in Coupled Nano-Layers", *International Journal of Non-Linear Mechanics*, Vol. **42** (4), pp. 681-689.

Raftoyiannis, I.G. and Kounadis, A.N., 2000, "Dynamic Buckling of 2-DOF Systems with Mode Interaction Under Step Loading", International Journal of Non-Linear Mechanics, Vol. 35, pp. 531-542.

Sophianopoulos, D.S., 2007, "Bifurcations and Catastrophes of a Two-Degrees-of-Freedom Nonlinear Model Simulation of the Buckling and Postbuckling of Rectangular Plates", Journal of the Franklin Institute, Vol. 344, pp. 463-488.

Teng, J.G. and Hong, T., 2006, "Postbuckling Analysis of Elastic Shells of Revolution Considering Mode Switching and Interaction", *International Journal of Solids and Structures*, Vol. **43** (3-4), pp. 551-568.

Thompson, J.M.T. and Gaspar, Z., 1977, "A Buckling Model for the Set of Umbilic Catastrophes", Math. Proc. Camb. Phil. Soc., Vol. 82, pp. 497.

Thompson, J.M.T. and Hunt, G.W., 1973, "A General Theory of Elastic Stability", John Wiley and Sons, London.

Thompson, J.M.T. and Hunt, G.W., 1984, "Elastic Instability Phenomena", John Wiley and Sons, London.

Thompson, J.M.T. and Stewart, H.B., 1987, "Nonlinear Dynamics and Chaos", John Wiley and Sons, London.

Tvergaard, V., 1973, "Imperfection-Sensitivity of a Wide Integrally Stiffened Panel Under Compression", *Int. J. Solids Structures*, Vol. **9**, pp. 177 - 192.

Vakakis, A.F., 1991, "Analysis and Identification of Linear and Nonlinear Normal Modes in Vibrating Systems", Doctoral Thesis, California Institute of Technology, Pasadena, USA.

Van der Heijden, A.M.A, 2008, "W. T. Koiter's Elastic Stability of Solids and Structures", Cambridge University Press, Cambridge, UK.

6. RESPONSIBILITY NOTICE

The authors are the only responsible for the printed material included in this paper.